A New Sensorless Commutation Technique for Brushless DC Motors[1]

D. Gambetta and A. Ahfock

Abstract

In brushless DC (BLDC) drives commutation is performed by power electronic devices forming part of an inverter bridge. Switching of the power electronic devices has to be synchronised with rotor position. Determination of position, with or without sensors is an essential requirement. The most common sensorless method is based on detection of the zero crossings of back EMF signals. This technique works only above a certain speed. BLDC systems which rely solely on back EMF signals for commutation suffer from relatively poor starting performance characterised by back rotation of up to one hundred and eighty electrical degrees and fluctuations in electromagnetic torque. The aim of this project has been to investigate the possibility of a sensorless technique which is cost effective but with a performance at start-up comparable with that obtained when Hall sensors are used. Initial investigations led to a saliency based method. Theoretical analysis is presented which shows that the method is insensitive to variations in operational parameters such as load current and speed or circuit parameters such as power device voltage drops and winding resistances. Also a starting strategy, relying on saliency related measurements, is proposed which offers starting performance as good as Hall sensor based techniques.

Keywords: brushless DC motors; sensorless commutation control

1. Introduction

[1] This paper is a postprint of a paper submitted to and accepted for publication in IET Electric Power Applications and is subject to Institution of Engineering and Technology Copyright. The copy of record is available at IET Digital Library. Doi: 10.1049/iet-epa:20070517

Fundamentally the brushless DC (BLDC) motor is very similar to the classical separately excited DC motor. Excitation for the latter is provided by windings or permanent magnets mounted on the stator. In the BLDC motor, excitation is provided by permanent magnets mounted on the solid iron rotor. The availability of cost-effective electronic control systems and high quality permanent magnets have increased the market share of BLDC motors. Neodymium-iron-boron (NdFeB) magnets are widely used in BLDC motors [1].

A number of methods are used to mount the magnets on the rotor [2]. The magnets may be surface mounted, surface inserted or they may be completely buried. With the latter construction method, unlike the other cases, the magnetic axis of the permanent magnets point in a substantially non-radial direction.

Reversal of direction of coil currents at precise rotor positions is essential in both conventional DC motors and in BLDC motors. In conventional motors this is carried out by means of the shaft mounted mechanical commutator and the brushes. The commutator and brushes act both as a set of switches to carry out current reversal and as a position sensor which ensures that the reversals are initiated at the right instants. In the BLDC motor electrical energy is fed to coils residing on the stator and excitation is provided by rotor mounted permanent magnets. Therefore there is no requirement for brushes and this is the most important advantage of BLDC motors compared to classical DC motors. There is still a requirement for stator coil current reversals to be synchronized with appropriate rotor positions. As in the case of the classical DC motor, this involves switching and position sensing. In the BLDC motor, however, switching and position detection are done separately. Switching is performed by power semiconductors, typically in a three-phase inverter bridge configuration using MOSFETs or IGBTs. This implies that BLDC motors are normally three-phase wound

with each motor line current controlled by one leg of the three-phase bridge. The inverter is operated in PWM mode with two out of the three phase windings energized at any one time [3]. Commutation between phases has to be performed every sixty electrical degrees. For optimum performance, commutation has to be carried out at precise rotor positions. Hall sensors are normally used if good commutation performance is essential right down to zero speed. Hall sensors also allow smooth start-up. However these sensors add cost and complexity especially in the case of small motors. Consequently there has been significant effort put into practical implementation of sensorless techniques for determination of commutation instants.

Sensorless position detection methods that have been proposed to date fall into two categories. There are those based on the use of on back EMF signals and those based on exploitation of saliency. Back EMF based methods are only applicable if speed is high enough. Nevertheless, there are many applications, for example drives for fans or pumps, that do not require position control or closed-loop operation at low speeds. For these, a back EMF based method is quite appropriate. Widely used, is the so called back EMF "zero crossing" method, where the zero crossing instants of the un-energised phase are used to estimate position [4]. It is important to mention that there is a 30° (electrical) offset between the back EMF zero-crossing and the required commutation instant, which must be compensated for to ensure correct operation of the motor.

BLDC motors which rely solely on back EMF signals for commutation suffer from relatively poor starting performance characterised by initial back rotation of up to one hundred and eighty electrical degrees and large fluctuations in electromagnetic torque resulting from non-ideal commutation instants. This may not be acceptable for certain applications and there have been attempts to develop sensorless techniques that give good performance right down to zero speed. Most of those attempts, while being saliency based, have been aimed at the brushless synchronous motor rather than the

BLDC motor [5-11]. Saliency based sensorless techniques for brushless synchronous motors are relatively complex because all the three phases are excited one hundred percent of the time. They rely on measurement of current and voltage responses to specially injected signals and require significant real time data processing. Ueki [12] and Weis [13] propose position detection techniques, based on saliency, specifically for BLDC motors and they reduce complexity by exploiting the availability of an unexcited phase. But they also rely on imposition of special signals onto the stator windings. Imposition of special signals requires additional electronics, can cause additional heating and deterioration of torque quality.

In this paper a sensorless method of detection of commutation instants is proposed which relies on inductive saliency. Unlike other proposed methods, no special signal injection is needed. The computational burden to deduce commutation instants is negligible. The technique is based on the detection of rotor positions where the two energised phases have equal inductances. It has therefore been termed the *equal inductance method* [14]. Gambetta [15] required a neutral connection for practical implementation of a version of the equal inductance method. It is shown in this paper that connection to the neutral is not necessary. Analytical results are presented which allow important deductions to be made about the robustness, sensitivity and resolution of the equal inductance method. Test results are presented which demonstrate practical application of the method.

An initial position detection and start-up method based on inductance measurement is also proposed and practically implemented.

2. Relationship between Equal Inductance Positions and Commutation Positions

Electrical machines that exhibit saliency may be analysed using the well established two-axis theory [16]. This theory leads to the following expressions for the three-phase winding inductances and mutual inductances:

$$L_{aa} = L_{aa0} + L_{al} + L_{g2}\cos(2\theta) \tag{1}$$

$$L_{bb} = L_{aa0} + L_{al} + L_{g2}\cos\left(2\theta + \frac{2\pi}{3}\right) \tag{2}$$

$$L_{cc} = L_{aa0} + L_{al} + L_{g2}\cos\left(2\theta - \frac{2\pi}{3}\right) \tag{3}$$

$$L_{ab} = L_{ba} = -0.5L_{aa0} + L_{g2}\cos\left(2\theta - \frac{2\pi}{3}\right) \tag{4}$$

$$L_{bc} = L_{cb} = -0.5L_{aa0} + L_{g2}\cos(2\theta) \tag{5}$$

$$L_{ac} = L_{ca} = -0.5L_{aa0} + L_{g2}\cos\left(2\theta + \frac{2\pi}{3}\right) \tag{6}$$

where θ is the electrical angle between the magnetic axis of phase A and the rotor direct axis or the rotor quadrature axis; L_{ii} is the self inductance of phase i; L_{ji} is the mutual inductance between phase i and phase j; L_{aa0}, L_{a1} and L_{g2} are positive constants which are independent of θ and, if the effects of saturation are ignored, they are also independent of winding currents. By definition the direct axis (d-axis) of the rotor is coincident with the magnetic axis of the rotor permanent magnet. The quadrature axis (q-axis) is ninety electrical degrees away from the d-axis.

Equations (1) to (6) are good representation of phase inductances of BLDC motors with surface mounted magnets or surface inset magnets. This conclusion was based on inductance measurements performed at 20 kHz or higher on a number of test machines. Fig. 1 shows the phase inductance profiles for one of those machines.

It is important to point out that the self-inductances and the mutual inductances that are referred to here are only effective values rather than actual values. The actual value of L_{aa}, for example, can only be obtained by measurement if all circuits that are magnetically linked to phase A were open-circuited. But that is not possible. Whilst the other two stator windings were open-circuited, the influence of eddy-currents in the magnets and other parts of the machine could not be eliminated. Thus the measured winding inductances are lower than their true values. They may be regarded as effective values that take into consideration the effect of eddy-currents, in a similar manner that the use of sub-transient inductances in synchronous machine analysis is a way of accounting for the effect of damper windings and other induced current paths on the rotor. In the case of the test motors, induced eddy currents in the magnets result in a lower phase inductance when the magnetic axis of that phase lines up with the magnetic axis of a rotor magnet (direct axis). Conversely, phase inductance is a maximum when the magnetic axis of the phase winding lines up with a quadrature axis. Thus the zero degree position in Fig. 1 or in table 1 corresponds to alignment of the phase A magnetic axis with the rotor quadrature axis.

The BLDC motor is normally operated with only two phases energised at any one time. Each phase is energised for a 120 electrical degree interval after which it is de-energised for a 60 electrical degree interval. The ideal commutation positions, θ_1 to θ_6, are shown in Table 1. These commutation positions lead to the highest electromagnetic torque per unit ampere as well as the lowest torque ripple. The reason for this is that each phase is energized during the 120 degree intervals centred about the peak value of the phase back EMF. There are six distinct commutation intervals. They have been labelled in Fig. 1 according to the phase pair that is energised and supply voltage polarity. For example CA corresponds to inverter transistors TB+ and TB-, shown in Fig. 2, being kept off and

the other four transistors switched so that, on average over a PWM cycle, phase terminal *c* is kept at a higher potential relative to phase terminal *a*.

It follows from the previous paragraph that the zero-crossings of the back EMF of a particular phase occurs 30 electrical degrees before that phase is energized. But the zero crossing of the back EMF of a phase winding also coincides with alignment of the magnetic axis of that winding with the d-axis of the rotor. Clearly at that position the self-inductance of that phase is a minimum, whereas the inductances of the two other phases will, because of geometric symmetry, be equal to each other. In other words, wherever the rotor d-axis aligns with the magnetic axis of the A-phase winding, back EMF E_a is equal to zero and $L_{bb} = L_{cc}$. Similar statements can be made about the B-phase winding and the C-phase winding. Thus the positions of equal inductance of the energized phases, just like the zero-crossings of the back EMF of the non-energised phase occur 30 electrical degrees before the next commutation position.

There are twelve positions of equal inductance over each electrical cycle (360 electrical degrees). Six of them correspond to the rotor q-axis coinciding with the magnetic axis of each one of the phase windings. The other six correspond to the rotor d-axis coinciding with the magnetic axis of each one of the phase windings. Only six of these, the ones associated with d-axis alignment will be used to help determine commutation positions. They are specified in Table 1.

3. Detection of Equal Inductance Positions

As mentioned before there are six commutation intervals. During each interval the aim is to have only two phases active. In Table 1 the six intervals have been labelled according to the phases that are active. Transition from one interval to the next involves de-energising of one phase and energising of the next one. This transition is complete only after the current in the outgoing phase has decayed to zero. Decay of the current occurs

through a diode and takes finite time. For example the transition from interval AC to interval BC involves decaying current through the diode D_A^-. Therefore each interval involves two sub-intervals, one during which all three-phase currents are present and one during which the non-active phase current is equal to zero. In total there are twelve sub-intervals and twelve corresponding inverter states. The inverter states are labelled according to the polarity of the DC supply terminal to which the motor phase terminals are connected. For example inverter state $c^+a^+ b^-$ implies the "c" and "a" phase terminals are connected, through transistors or diodes to the positive DC rail whereas the "b" terminal is connected to the negative DC rail. Since bipolar PWM is used, during any one of the commutation intervals, the inverter may be in one of six possible states. For example during interval AB, the inverter may be in state $a^+c^+b^-$, or $a^+c^-b^-$, or $a^-c^+b^+$, or $a^-c^-b^+$, or a^+b^-, or b^+a^-.

The aim is to use inductive saliency to determine the correct commutation instants for the motor. The method is based on the sensing of the potential at the non-energised phase winding terminal after the current in that phase has decayed to zero. Consider commutation interval AB. Assuming current i_c has decayed to zero, the inverter will revert alternately between the states a^+b^- and b^+a^-. These are represented by the equivalent circuits in Fig. 3.

Voltage measurements v_{cy}^+ and v_{cy}^- are carried out while the inverter is respectively in states a^+b^- and b^+a^-. For consistency, as shown in Fig. 4, measurements are carried out near the middle of the applied voltage pulses. Consecutive measurements v_{cy}^+ and v_{cy}^- are compared. It is shown, in the next paragraphs that those two values are equal to each other at precisely the position of equal inductance independent of the value of phase current, supply voltage or speed. Thus, by cyclic monitoring of voltage signals v_{cy}, v_{ay}

and v_{by}, commutation instants can be pre-determined with very little computational effort.

Consider operation during commutation interval AB. With the inverter in state a^+b^- we have:

$$v_{sy}^{+} = \frac{1}{2}\left(V_{dc} - v_{ay}^{+}\right) - \frac{1}{2}v_{by}^{+} \tag{7}$$

Since $i_a = -i_b$, equation (7) gives:

$$v_{sy}^{+} = \frac{V_{dc}}{2} + \left(\frac{L_{bb} - L_{aa}}{2}\right)\left(\frac{di_a}{dt}\right)^{+} + \frac{i_a}{2}\frac{d\left(L_{bb} - L_{aa}\right)}{dt} - \left(\frac{E_b + E_a}{2}\right) \tag{8}$$

Adding v_{cs}^{+} to v_{sy}^{+} yields:

$$v_{cy}^{+} = \frac{V_{dc}}{2} + \left(\frac{L_{bb} - L_{aa} + 2L_{ca} - 2L_{cb}}{2}\right)\left(\frac{di_a}{dt}\right)^{+} + \frac{i_a}{2}\frac{d\left(L_{bb} - L_{aa} + 2L_{ca} - 2L_{cb}\right)}{dt} - \left(\frac{E_a + E_b - 2E_c}{2}\right) \tag{9}$$

Also,

$$\left(\frac{di_a}{dt}\right)^{+} = \frac{\left(V_{dc} - i_a \frac{d\left(L_{aa} + L_{bb} - 2L_{ab}\right)}{dt} - E_a + E_b - 2V_t^{+} - 2i_a R\right)}{\left(L_{aa} + L_{bb} - 2L_{ab}\right)} \tag{10}$$

where $2V_t^{+}$ is the total switching device voltage drop.

With the inverter in state $b^{+}a^{-}$ we have:

$$v_{sy}^{-} = \frac{1}{2}\left(V_{dc} - v_{by}^{-}\right) - \frac{1}{2}v_{ay}^{-} \tag{11}$$

Since i_a=-i_b, equation (11) gives:

$$v_{sy}^{-} = \frac{V_{dc}}{2} + \left(\frac{L_{bb} - L_{aa}}{2}\right)\left(\frac{di_a}{dt}\right)^{-} + \frac{i_a}{2}\frac{d\left(L_{bb} - L_{aa}\right)}{dt} - \left(\frac{E_b + E_a}{2}\right) \tag{12}$$

Adding v_{cs}^{-} to v_{sy}^{-} yields:

$$v_{cy}^{-} = \frac{V_{dc}}{2} + \left(\frac{L_{bb} - L_{aa} + 2L_{ca} - 2L_{cb}}{2}\right)\left(\frac{di_a}{dt}\right)^{-} + \frac{i_a}{2}\frac{d\left(L_{bb} - L_{aa} + 2L_{ca} - 2L_{cb}\right)}{dt} - \left(\frac{E_a + E_b - 2E_c}{2}\right) \tag{13}$$

Also,

$$\left(\frac{di_a}{dt}\right)^{-} = \frac{\left(-V_{dc} - i_a \frac{d\left(L_{aa} + L_{bb} - 2L_{ab}\right)}{dt} - E_a + E_b - 2V_t^{-} - 2i_a R\right)}{\left(L_{aa} + L_{bb} - 2L_{ab}\right)} \tag{14}$$

where $2V_t^-$ is the total switching device voltage drop. There may be a small difference between V_t^+ and V_t^- because, for example, in the a^+b^- state a pair of inverter transistors may be conducting whereas in b^+a^- state it may be a pair of inverter diodes that carries the phase currents.

In equations 7 to 14 superscript "+" denotes values sampled while the inverter in the a^+b^- state (t_s^+ in Fig. 4) whereas the superscript "-" denotes values sampled while the inverter is in the b^+a^- state (t_s^- in Fig. 4). If PWM frequency is high enough and speed is low enough, then it is reasonable to assume that there is negligible change in currents, inductances and back emfs from time t_s^+ to time t_s^-. Therefore no superscripts have been used for those variables.

If the reasonable assumption is made that (V_t^+ - V_t^-) is negligible compared to V_{dc}, it can be deduced from equations 9, 10, 13 and 14 that:

$$v_{cy}^+ - v_{cy}^- = V_{dc}\left(\frac{L_{bb} - L_{aa} + 2L_{ca} - 2L_{cb}}{L_{aa} + L_{bb} - 2L_{ab}}\right) \tag{15}$$

Equation 15 confirms that, independent of all operating and machine parameters, the rotor position at which v_{cy}^+ and v_{cy}^- are equal coincides with the position equal inductance ($L_{aa} = L_{bb}$ and $L_{ca} = L_{cb}$).

Equation 15 may be written as:

$$v_{cy}^{+} - v_{cy}^{-} = \frac{V_{dc}\left(\sqrt{3}\left(L_q - L_d\right)\cos\left(2\theta + \frac{5\pi}{6}\right)\right)}{\left(L_q + L_d + (L_q - L_d)\cos\left(2\theta + \frac{\pi}{3}\right)\right)} \tag{16}$$

where:

$$L_q = L_{al} + \frac{3}{2}\left(L_{aa0} + L_{g2}\right) \tag{17}$$

and

$$L_d = L_{al} + \frac{3}{2}\left(L_{aa0} - L_{g2}\right) \tag{18}$$

For reasonable saliency ratios, of say less than 1.2, a good approximation for $(v_{cy}^{+} - v_{cy}^{-})$ is:

$$v_{cy}^{+} - v_{cy}^{-} = \frac{V_{dc}\left(\sqrt{3}\left(S-1\right)\cos\left(2\theta + \frac{5\pi}{6}\right)\right)}{\left(S+1\right)} \tag{19}$$

where S is the saliency ratio.

Similarly:

$$v_{ay}^{+} - v_{ay}^{-} = \frac{V_{dc}\left(\sqrt{3}(S-1)\cos\left(2\theta - \frac{\pi}{2}\right)\right)}{(S+1)} \tag{20}$$

and

$$v_{by}^{+} - v_{by}^{-} = \frac{V_{dc}\left(\sqrt{3}(S-1)\cos\left(2\theta + \frac{\pi}{6}\right)\right)}{(S+1)} \tag{21}$$

It is deduced from equation 19 (or 20 or 21) that the sensitivity and precision of the equal inductance method of pre-determination of commutation instants is dependent only on saliency ratio and the DC supply voltage. Fig. 5 represents practical confirmation of equation 19 to 21.

4. Initial Position Detection and Start-Up

Assuming the rotor is initially at standstill, the start-up procedure using the newly proposed sensorless method consists of the following steps:

(a) Determine, by solving any two of equations 19 to 21, the two possible values for θ_i, the rotor initial position.
(b) Identify the phase pair that on energisation will provide the maximum driving torque.
(c) Energise the selected phase pair until θ_i changes by a small (typically less than one mechanical degree) but measurable amount.
(d) Depending on whether θ_i increased or decreased in step (c), determine the actual value of θ_i.
(e) Use one of equations 19 to 21 to evaluate P where:

$$P = \frac{V_{dc}\sqrt{3}(S-1)}{(S+1)} \tag{22}$$

(f) Identify the phase pair and polarity that will provide maximum driving torque for rotation in the desired direction.

(g) Energise the phase pair identified in step (f) and initiate commutation to the next phase pair when the value of the measured voltage difference (left hand side of equation 19 or 20 or 21) reaches $\sqrt{3}P/2$.

(h) Activate the normal commutation algorithm straight after initiation of the first commutation event.

Step (a) requires at least two phase pair energisations to be done with 50 percent PWM to avoid rotation. Any two or more of the six possible phase pair combinations could be used. A good strategy would be to use the three pairs and polarities corresponding to equations 19 to 21 and select two for the determination of θ_i. The third equation can be used for verification purposes. If, for example, equations 19 and 20 were chosen to determine the rotor initial position θ_i, then we have:

$$\theta_d = \tan^{-1}(P_s / P_c) \tag{23}$$

where:

$$\begin{pmatrix} P_s \\ P_c \end{pmatrix} = \begin{pmatrix} P\sin(2\theta_i) \\ P\cos(2\theta_i) \end{pmatrix} = \begin{pmatrix} -1/2 & -\sqrt{3/2} \\ 1 & 0 \end{pmatrix}^{-1} \begin{pmatrix} v_{cy}^{+} - v_{cy}^{-} \\ v_{ay}^{+} - v_{ay}^{-} \end{pmatrix} \tag{24}$$

In applying equations 19 to 24 together with measured voltage differences ($v_{cy}^{+} - v_{cy}^{-}$) and ($v_{ay}^{+} - v_{ay}^{-}$), a unique value for θ_d is obtained in the zero to 360 electrical degree range. The initial rotor position θ_i, however is either equal to $\theta_d/2$ or $\theta_d/2$ plus 180 electrical degrees. The purpose of steps (b), (c) and (d), listed above, is to determine whether θ_i is equal to $\theta_d/2$ or to $(\theta_d + 2\pi)/2$. The phase pair combination to be selected in step (b) should be according to the following:

CA if $0^\circ \leq \theta_d / 2 \leq 60^\circ$;

CB if $60^\circ \leq \theta_d / 2 \leq 120^\circ$; and

AB if $120^\circ \leq \theta_d / 2 \leq 180^\circ$.

During step (c) the PWM duty ratio is deviated from 50% just enough to allow a small but measurable change in θ. If θ increases then it can be deduced that $\theta_i = \theta_d / 2$ otherwise it is concluded that $\theta_i = (\theta_d + 2\pi) / 2$.

Step (f) is about choosing the optimum phase pair for initial movement in the right direction. This can be done according to table 1. For example, if the motor initial position is between 60° and 120° and backward rotation was desired, then the phase pair to be energised should be BC. After the first commutation event, performed according to step (g) above, subsequent commutation control is carried out by executing the algorithm in Fig. 6.

5. Test Results

BLDC commutation based on the equal inductance method was implemented and tested on a motor whose nameplate data is given in table 2. The commutation algorithm was implemented using the 56F8013 digital signal controller [17].

As shown in Fig. 7 there is good agreement between the standstill rotor positions deduced by solving two of equations 19 to 21 and the actual rotor position. This is in spite of the existence of a small imbalance in phase inductances. The maximum deviation between actual position and estimated position was found to be 1.4 electrical degrees.

Fig. 8 shows oscillograms of phase A voltage (v_{ay}), phase A current, the *equal inductance flag* and the *commutation flag*. The control software operates such that the *equal inductance flag* changes state whenever the rotor passes through a position where the energised phases have equal inductances. Thus, as expected, the *equal inductance flag* changes state every 60 electrical degrees. By design the *commutation flag* lags the equal inductance flag by 30 electrical degrees. The waveforms in Fig. 8 confirm correct commutations since commutation events occur every sixty electrical degrees and disturbance of the non-commutating phase current is small. Fig. 9 confirms that the equal inductance method works well at higher current and higher speed.

The equal inductance method is used to pre-determine all commutation instants except the first one. The *first commutation flag*, displayed in Fig. 10, is set when the voltage difference (left hand side of equation 19 or 20 or 21) reaches the pre-calculated value of $\sqrt{3}P/2$. The test results in Fig. 10 confirm correct operation of the proposed starting

method since the timing of the instant of the first commutation event determined by the *first commutation flag* is consistent with the timing of subsequent commutation event which are determined by the normal *commutation flag*.

6. Discussion

Performance of the *equal inductance method* is best near zero speed since both positive and negative PWM voltage pulses applied to the active phase pair are relatively wide. Under those conditions, there is sufficient time for transients to settle before measurements are made. Also there is sufficient time to perform computations. However, as speed rises either the positive voltage pulse or the negative pulse within a PWM cycle becomes shorter and eventually there may not be sufficient time for transients to settle and for calculations to be performed. Thus there exists an upper limit of satisfactory performance of the *equal inductance method*. It is not possible to arrive at a general conclusion regarding this limit. It depends on supply voltage, saliency, resolution and speed of the selected digital signal processor and the effect of switching noise. With a saliency ratio of 1.1 or more, 12V DC supply and a low cost DSP with 8-bit resolution, it is estimated that performance as good as that obtained with the back EMF zero crossing is achievable at about 25% of full speed. Well above that speed the back EMF method is better, whereas well below that speed the equal inductance method gives superior performance. Thus the *equal inductance method* complements the back EMF very well.

The *equal inductance method* is based on voltage measurements made as voltage pulses are applied to active winding pairs during bipolar operation. There is no practical advantage in adapting the method to unipolar operation. With unipolar operation, correct measurement at very low speed is not possible because the voltage pulse width is too

short. Thus adapting the *equal inductance method* to unipolar operation will not result in a technique that complements the back EMF zero crossing method. If unipolar operation is preferred for normal motor operation, it is recommended that the motor is started under bipolar operation and the *equal inductance method* up to a minimum speed. Above that speed, operation can be changed to unipolar with back EMF zero crossings used to determine commutation instants.

The *equal inductance method* has been found to perform very well with motors having surfaced inserted magnets. However, the method can be considered for motors with fully buried magnets. Qualitative analysis suggests that these motors would exhibit inductive saliency due to the cumulative effects of rotor geometry and eddy currents induced in their permanent magnets.

7. Conclusions

A low cost saliency based sensorless technique for BLDC motors has been proposed, physically implemented and tested. It offers performance that is equal to that obtained by systems relying on low resolution physical devices such as Hall sensors. Rotor position is deduced from the response of the BLDC motor un-energised phase terminal voltage, measured with respect to the negative DC supply rail, due to bipolar PWM voltage pulses that are normally applied to the other two phases. Theoretical analysis shows that this potential difference is made up of a DC component equal to the sum of half the DC supply voltage and the un-energised phase back EMF plus an AC component (non-sinusoidal) that is modulated by the rotor movement. In other words the peak to peak value of the AC component varies as rotor position changes. The fundamental frequency of the AC component is equal to the PWM frequency. It was found, from the theoretical investigation, that a zero peak to peak value of the AC component corresponds to a rotor position that is thirty electrical degrees away from the next ideal commutation position. That rotor position is also the one where the energized

phase windings have equal inductances. Hence the adopted sensorless commutation control method has been termed the ‘equal inductance method’. Further theoretical analysis showed that the peak to peak value of the AC component depends only on the DC supply voltage and the saliency ratio. In other words the position of equal inductance deduced from voltage measurements at the un-energised phase terminal is insensitive to operational parameters such as load current and circuit parameters such as winding resistance.

It has been demonstrated that with sufficient saliency, standstill rotor position can be determined from the same measurements made to determine positions of equal inductance. The necessary phase winding energisations during those measurements may lead to some back-rotation. But this has been found to be less than a mechanical degree and is therefore considered negligible. Once the initial rotor position has been determined, the optimum phase pair to be energised can be selected. Voltage measurements allow the rotor position for the first commutation event to be identified, subsequent commutation instants being pre-determined by the ‘equal inductance method’.

The back EMF method of commutation control relies on detection of zero-crossing instants of the back EMF signal from the unenergised phase. It has been shown that the instant at which the rotor reaches the equal inductance position coincides with the zero-crossing instant of the back EMF of the unenergised phase. There is, therefore, a close parallel between the equal inductance method and the back EMF method. For operation over a wide speed range it may be advantageous to operate using the equal inductance method at low speed and the back EMF method at high speed. The close parallel between the two methods makes it easy to implement changeover strategies from one to the other as the motor speed crosses the chosen boundary between low speed and high speed operation.

In summary the *'equal inductance method'* is easy to implement, is very cost competitive and offers commutation and starting performance equal to that obtained with Hall sensors. Also, its close parallel with the back EMF method allows seamless changeover to that method at high speeds.

Acknowledments

The authors would like to acknowledge that this paper reports outcomes of a project that has been carried out with financial support provided by Metallux SA, Mendrisio, Switzerland.

7. References

[1] Krishnan R.,'*Electric motor drives: modelling, analysis and control'*, Prentice Hall, Upper Saddle River, USA, 2001.

[2] Miller T J E.,'*Brushless Permanent-Magnet and Reluctance Motor Drive',* Oxford University Press, Oxford,UK, 1989.

[3] Valentine R. '*Motor control electronics handbook'*, first edition, McGraw Hill, Singapore, 1998.

[4] Prokop L, '*3-phase BLDC motor control with sensorless back-EMF ADC zero crossing detection using the 56F805, Designer reference manual'*, Motorola Czech System Laboratories, Roznov pod Radhostem, Czech Republic, 2003

[5] Bolognani S., Oboe R. and Zigliotto M, *'Sensorless full-digital PMSM drive with EKF estimation of speed and rotor position'*, IEEE Transaction on Industrial Electronics, Volume 46, Issue 1,1999, pp. 184-191

[6] Kim S. and Sul S, *'New approach for high-performance PMSM drives without rotational position sensors'*, IEEE Transaction on Power Electronics,Volume 12, Issue 5, 1997, pp. 904-911

[7] Petrovic V., Stankovic A. and Blasko V, *'Position estimation in salient PM synchronous motors based on PWM excitation transients'*, IEEE Transaction on Industry Applications, , Volume 39, Issue 3, 2003, pp. 835-843

[8] Robeischl E. and Schroedl M, *'Optimized INFORM measurement sequence for sensorless PM synchronous motor drives with respect to minimum current distortion'*, IEEE Transaction on Industry Applications, , Volume 40, Issue 2, 2004, pp. 591-598

[9] Schmidt P., Gasperi M., Ray, G. and Wijenayake A, *'Initial rotor angle detection of a non-salient pole permanent magnet synchronous machine'*, IEEE Industry Applications Society Annual Meeting, New Orleans,1997

[10] Shouse K. and Taylor D, *'Sensorless velocity control of permanent-magnet synchronous motors'*, IEEE Transaction Control System Technology, Volume 6, Issue 3,,1998, pp. 313-324

[11] Wang L., Lorenz R.,*'Rotor Position Estimation for Permanent Magnet Synchronous Motor Using Saliency-Tracking Self-Sensing Method'*, Proceedings.of IEEE IAS Annual Meeting, Rome, Italy, 2000, pp. 445-450

[12] Ueki Y, *'Detection of relative position between magnetic pole and drive coil in brushless dc motor'*, United State Patent, Patent Number 5,159,246,1992

[13] Weiss W,*'Artificial heart with sensorless motor'*, United State Patent, Patent Number 5,751,125, 1998

[14] Ahfock A., and Gambetta D., '*Technique for Sensorless Commutation of Brushless DC Motors* ', Swiss Institute of Intellectual Property, Bern, Patent Application Number 00342/05, 2005.

[15] Gambetta D., '*Sensorless Technique for BLDC Motors*', MPhil Dissertation, University of Southern Queensland, Australia, 2006

[16] Fitzgerald, A., Kingsley, C. and Umans, S, *Electric machinery*, sixth edition, McGraw Hill, Singapore, 2003

[17] Freescale Semiconductor, *56F8000 16-bit digital signal controller peripheral reference manual*, rev 0, 2005, Freescale Semiconductor Literature Distribution Center, Denver, USA

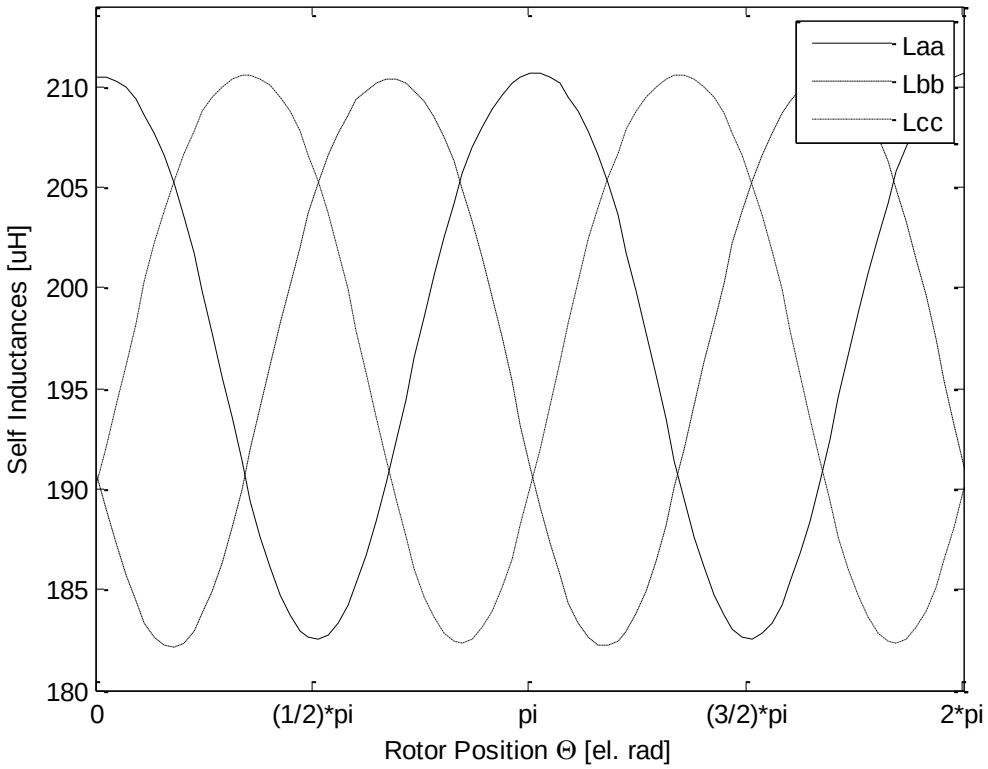

Fig. 1: Measured Self-Inductances

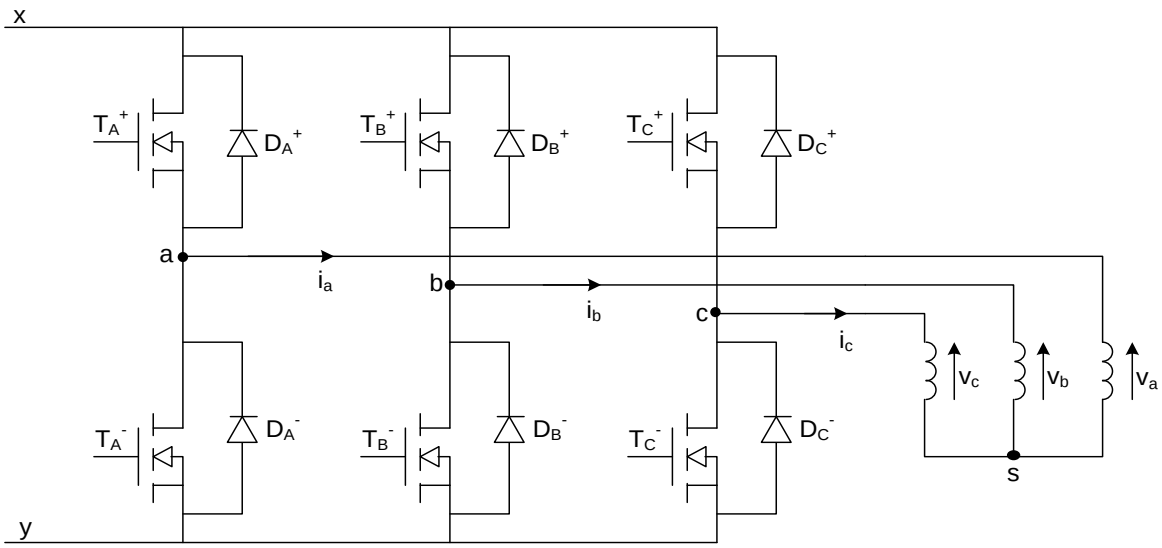

Fig. 2: Inverter Bridge Supplying a Brushless DC Motor

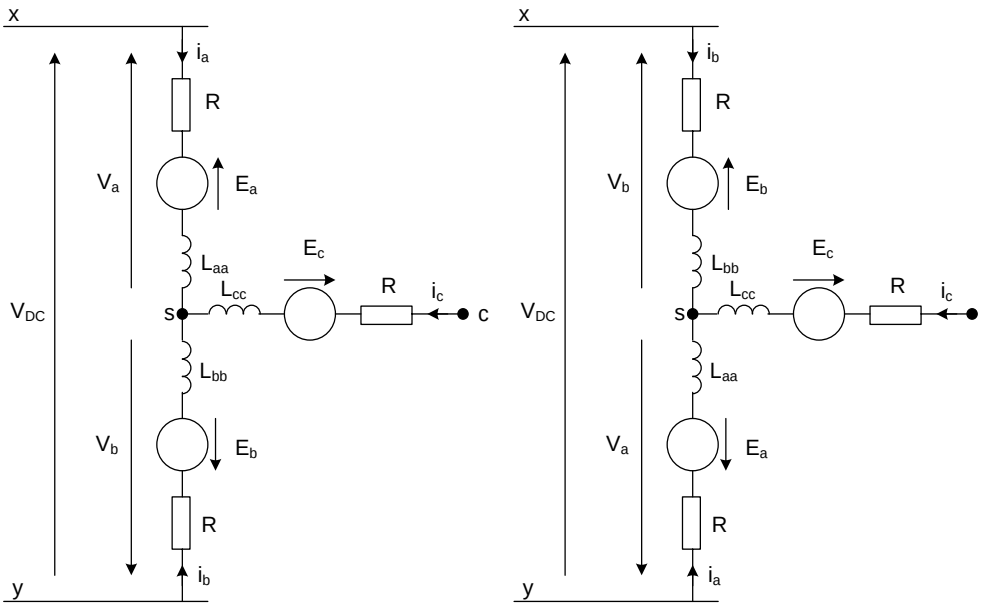

Fig. 3: Equivalent circuits for inverter states a^+b^- and b^+a^-
(switching device voltage drop not shown)

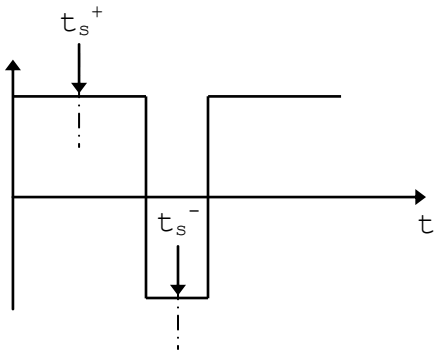

Fig. 4: Voltage Sampling Instants (t_s^+ and t_s^-)

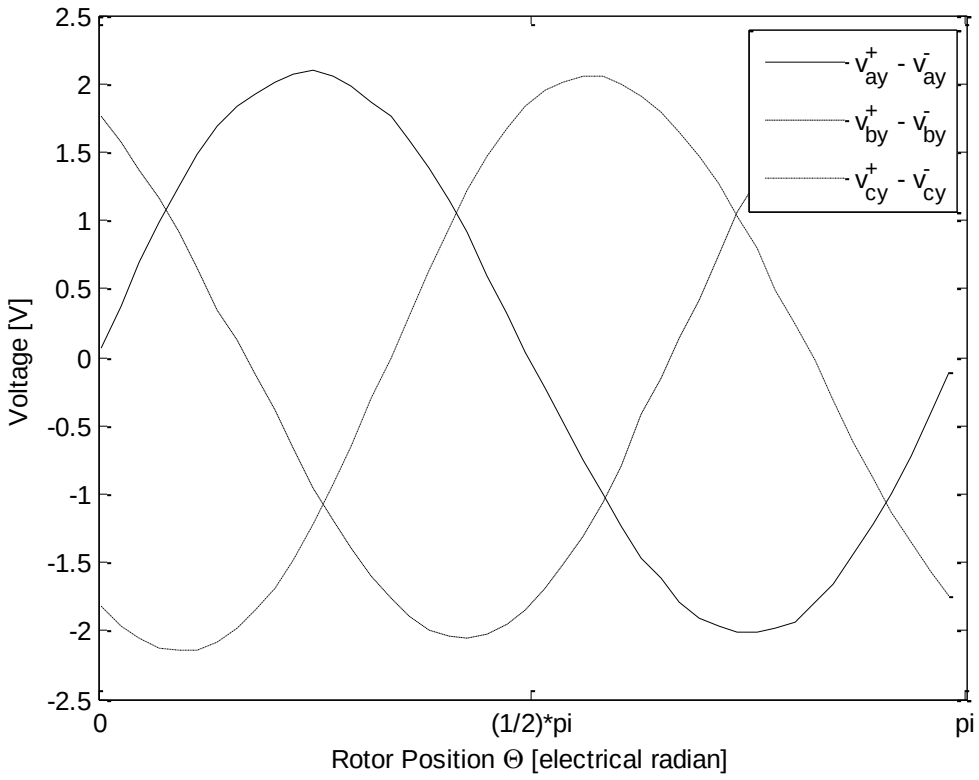

Fig. 5: Measured Voltage Differences (eqs 19 - 21)

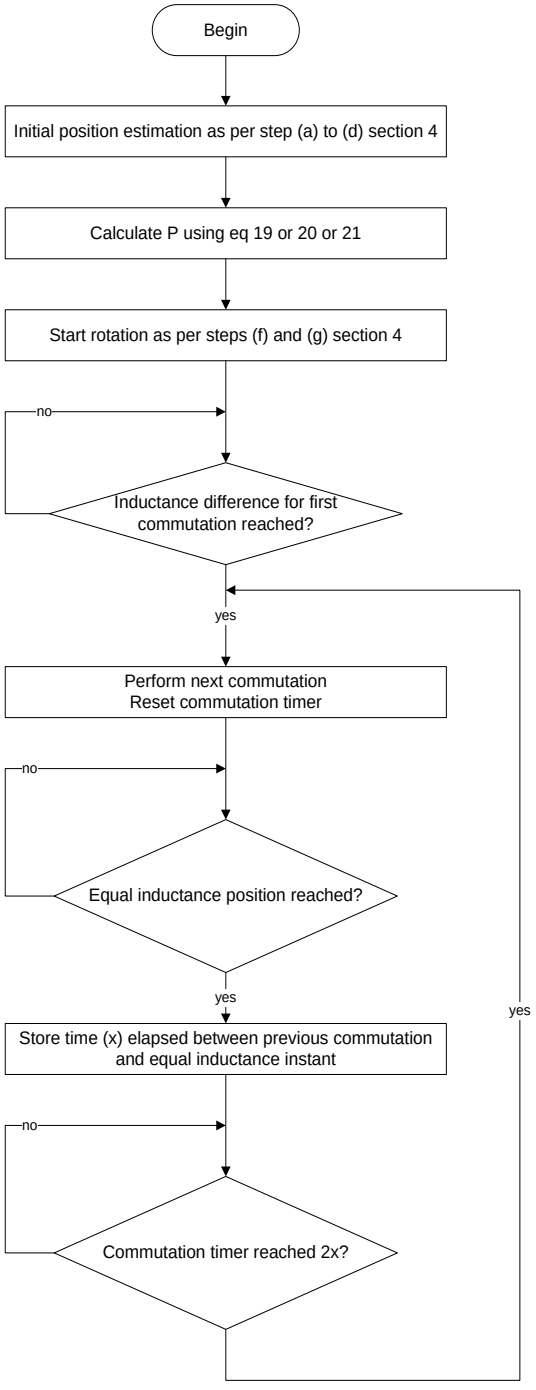

Fig. 6: Commutation Algorithm Based on the Equal Inductance Method

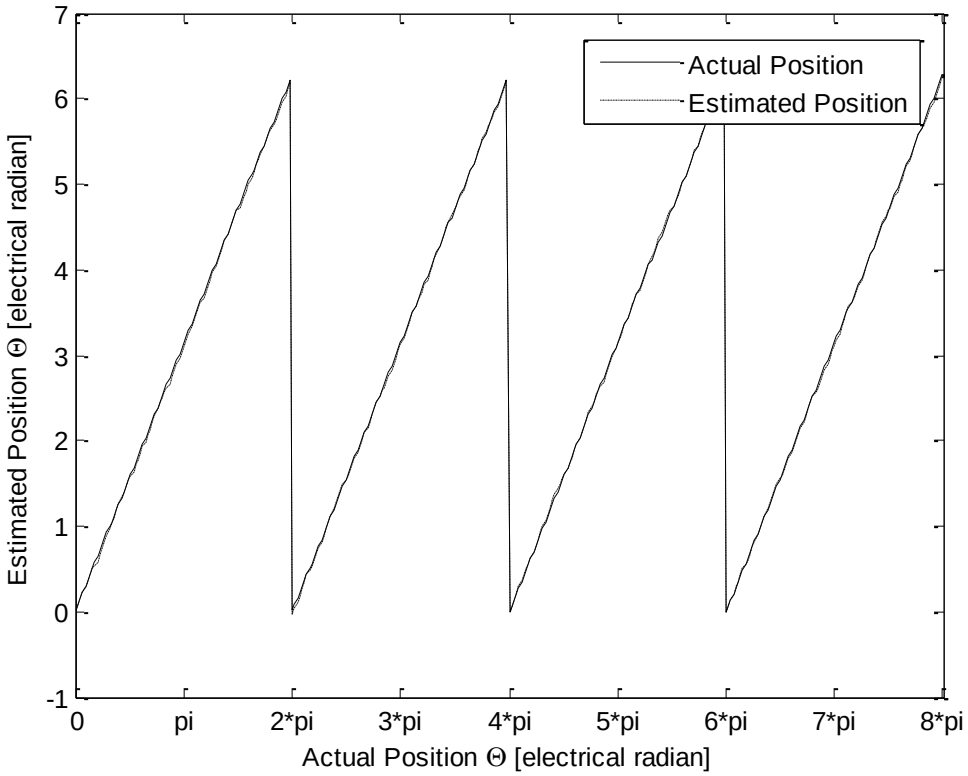

Fig. 7: Comparison between Actual and Estimated Rotor Position (360° Mechanical)

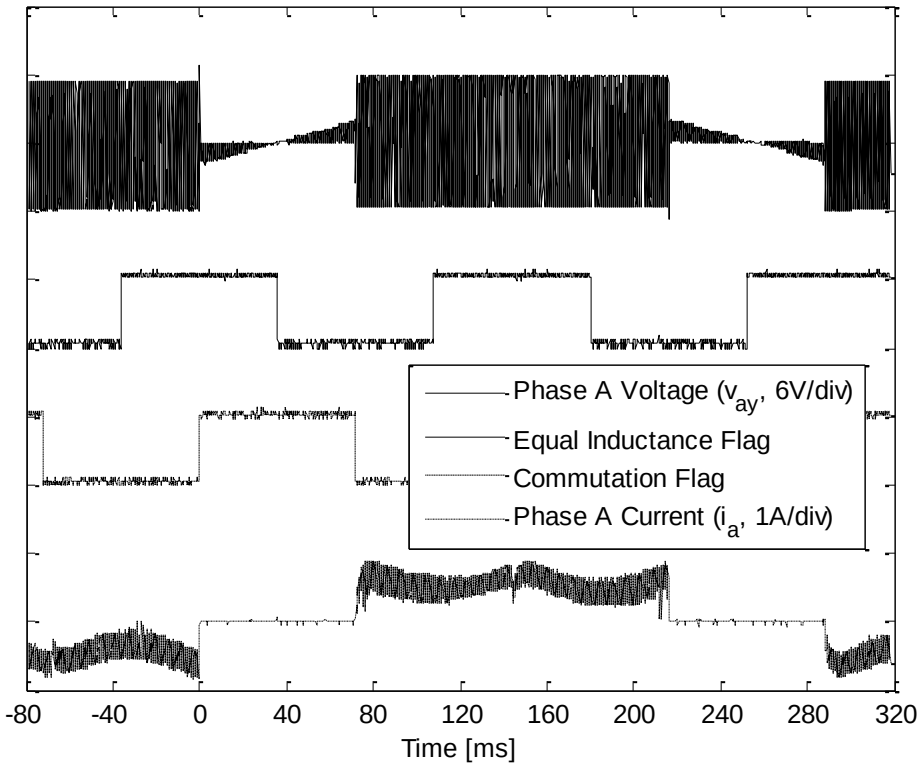

Fig. 8: BLDC Commutation using the Equal Inductance Method (139 r/min)

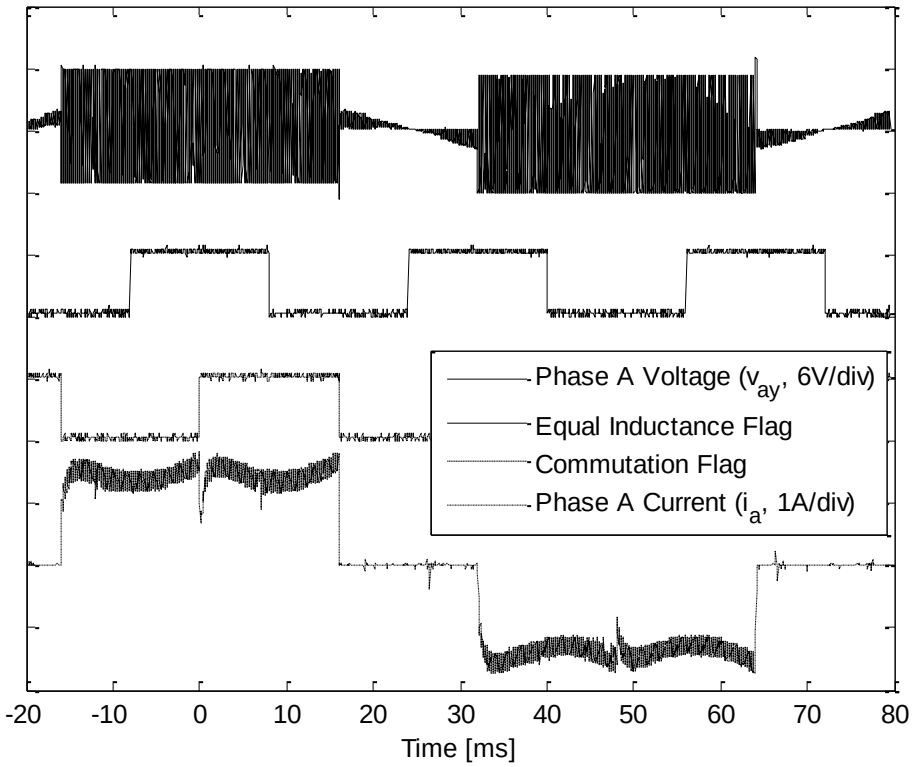

Fig. 9: BLDC Commutation using the Equal Inductance Method (630 r/min)

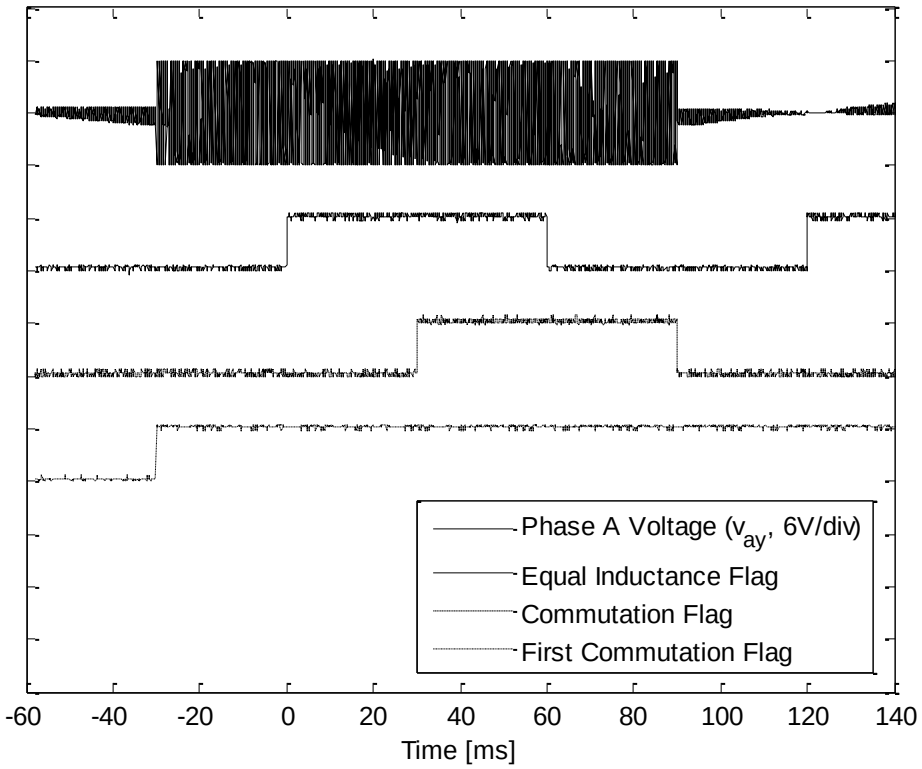

Fig. 10: First Commutation Event

Table 1: Equal Inductance Positions and Commutation Intervals

Rotor position range (electrical degrees)	0° to 60°	60° to 120°	120° to 180°	180° to 240°	240° to 240°	300° to 360°
Energised pair in each commutation interval	CA	CB	AB	AC	BC	BA
Equal inductance position before next commutation event	30°	90°	150°	210°	270°	330°
Next commutation position	$\theta_1 =$ 60°	$\theta_2 =$ 120°	$\theta_3 =$ 180°	$\theta_4 =$ 240°	$\theta_5 =$ 300°	$\theta_6 =$ 360°

Table 2: Test Motor Details

Rated Voltage (V)	12
Rated Current (A)	2
Rated Speed (rpm)	2400
Number of Poles	8